ISSN 1343-2230
CNS-REP-67
ISSN 1346-244X
RIKEN-AF-NP-469
October, 2005

CNS **CNS Report**

Proton Single-Particle States in the Neutron-rich ^{23}F Nucleus

S. Michimasa, S. Shimoura, H. Iwasaki, M. Tamaki, S. Ota, N. Aoi, H. Baba, N. Iwasa, S. Kanno, S. Kubono, K. Kurita, M. Kurokawa, T. Minemura, T. Motobayashi, M. Notani, H.J. Ong, A. Saito, H. Sakurai, E. Takeshita, S. Takeuchi, Y. Yanagisawa, A. Yoshida

Submitted to Physics Letters B

Center for Nuclear Study (CNS)

Graduate School of Science, the University of Tokyo
Wako Branch at RIKEN, 2-1 Hirosawa, Saitama 351-0198, Japan
Correspondence: cnsoffice@cns.s.u-tokyo.ac.jp

Proton Single-Particle States in the Neutron-rich ^{23}F Nucleus

S. Michimasa [a], S. Shimoura [b], H. Iwasaki [c], M. Tamaki [b], S. Ota [d], N. Aoi [a], H. Baba [a], N. Iwasa [e], S. Kanno [f], S. Kubono [b], K. Kurita [f], M. Kurokawa [a], T. Minemura [a], T. Motobayashi [a], M. Notani [b,1], H.J. Ong [c], A. Saito [b], H. Sakurai [a], E. Takeshita [f], S. Takeuchi [a], Y. Yanagisawa [a], A. Yoshida [a]

[a] *RIKEN (The Institute of Physical and Chemical Research), 2-1 Hirosawa, Wako, Saitama 351-0198, Japan*

[b] *Center for Nuclear Study, University of Tokyo, RIKEN campus, 2-1 Hirosawa, Wako, Saitama 351-0198, Japan*

[c] *Department of Physics, University of Tokyo, 7-3-1 Hongo, Bunkyo, Tokyo 113-0033, Japan*

[d] *Department of Physics, Kyoto University, Kitashirakawa, Kyoto 606-8502, Japan*

[e] *Department of Physics, Tohoku University, Aoba, Sendai, Miyagi 980-8578, Japan*

[f] *Department of Physics, Rikkyo University, 3-34-1 Nishi-Ikebukuro, Toshima, Tokyo 171-8501, Japan*

Abstract

Preprint submitted to Elsevier Science *18 October 2005*

The proton shell structure in neutron-rich fluorine ^{23}F was investigated using the in-beam γ-ray spectroscopy technique via the proton transfer reaction onto the unstable ^{22}O nucleus. We also measured the α inelastic scattering on ^{23}F, neutron knockout from ^{24}F, and two-nucleon knockout from ^{25}Ne using a cocktail secondary beam. By comparison of the population strengths for excited states in these reactions, we deduced the character of the excited states. The levels and γ-decay scheme in ^{23}F were deduced from de-excitation γ-rays and the products of these reactions. We found that the 2268- and 4059-keV levels have strong proton single-particle nature of the $s_{1/2}$ and $d_{3/2}$ orbitals, respectively, by analysis of the population strengths and the angular distributions of states. These single-particle states are located at higher excitation energies than shell model predictions for the USD and SDPF-M interactions, which indicates that the centroid energy gaps for $\pi d_{5/2}$–$\pi s_{1/2}$ and $\pi d_{5/2}$–$\pi d_{3/2}$ are wider than those for the predictions.

Key words: α-Induced stripping reactions, γ-Ray spectroscopy, Single-particle states

PACS: 21.10.Pc, 25.55.Hp, 27.30.+t, 29.30.Kv

One of the most ambitious challenges in studies of neutron-rich nuclei is to clarify the underlying nuclear interactions by disclosing the nuclear structure from the stability line to the drip line. In this respect, neutron-rich oxygen and fluorine isotopes are very fascinating subjects. In these isotopes, exotic phenomena have been observed, such as the new magic numbers at $N = 16$ [1], the sudden change in the neutron drip line from $Z = 8$ to $Z = 9$ [2] and a nuclear deformation region in spite of $N = 20$, i.e., the so-called island-of-

Email address: mitimasa@riken.jp (S. Michimasa).

[1] Present address: Physics Division, Argonne National Laboratory, Argonne IL60439, USA

inversion region [3]. To date, these phenomena have been discussed in terms of the nuclear structure, focusing on the configuration of valence neutrons. As one possible interpretation based on the shell model, shell evolution of the neutron orbitals caused by a two-body effective interaction between the valence neutron and the valence proton [4] was proposed. On the other hand, shell evolution of the proton orbitals has rarely been discussed, although the two-body effective interaction affects the protons as well as the neutrons. Investigations of the proton shell structure in these nuclei may yield a great opportunity to reveal new properties of an asymmetric nuclear system, since the valence proton is more deeply bound than those in stable nuclei.

We report here an experimental study of the structure of the ^{23}F nucleus using the proton stripping reaction onto the neutron-rich unstable ^{22}O nucleus in the inverse kinematics. Since ^{23}F has the ^{22}O plus one proton system, in which the core has the proton magic number of $Z = 8$ and neutron sub-shell closure of $N = 14$, it is appropriate for the study of proton single-particle orbitals. By comparison of the excitation-level structures in ^{17}F, which has the ^{16}O plus one proton system, we expected to observe changes in the proton single-particle orbitals because of the difference between full and empty occupancy of the neutron $d_{5/2}$ orbital, or rather, the difference in binding energy of the valence protons. In particular, it would be interesting to find a single-particle state attributed to the proton $d_{3/2}$ orbital, because its excitation energy is directly affected by the spin–orbit splitting between the d orbitals, in which the spin–isospin monopole interaction is suggested to play a major role [4].

To identify experimentally the proton single-particle states in ^{23}F, we compared the population strengths of the excited states in ^{23}F from four α-induced direct reactions: the one-proton transfer reaction onto ^{22}O; the α inelastic scat-

tering of ^{23}F; neutron knockout from ^{24}F; and two-nucleon knockout from ^{25}Ne. Such a comparison is appropriate for identifying single-particle states among the many excited states, since the cross-sections of these reactions are considered to depend on the characteristics of each excited state. These reactions were simultaneously observed using a cocktail beam in the vicinity of ^{23}F at intermediate energy and a liquid helium target [5]. The liquid helium target was chosen because of the statistical advantage of the reaction yields. It is noted that the (α,t) reaction has a relatively large cross-section (order of mb) in the intermediate energy region. This feature originates from the fact that a proton constituting an α particle is deeply bound and has a high-momentum component, so that the momentum mismatch of the (α,t) reaction is reduced for neutron-rich unstable nuclei. The excited states in ^{23}F were identified by measuring de-excitation γ-rays coincident with the outgoing ^{23}F. Since some of the excited states decay through γ-ray cascades, these were identified by coincidence γ-ray analysis.

The experiment was performed at the secondary-beam line in the RIKEN Accelerator Research Facility. The secondary beam, including ^{22}O, ^{23}F, ^{24}F and ^{25}Ne, was produced by projectile fragmentation reactions of a 63A-MeV ^{40}Ar beam impinging on a ^{9}Be production target of 180 mg/cm^2. Fragments were analyzed by a RIPS separator [6] using a wedge aluminum degrader of 321 mg/cm^2 at the first dispersive focal plane, where the momentum acceptance was set to 4%. Secondary beam particles were identified event-by-event according to the energy loss signals from a silicon detector and the time of flight between two plastic scintillators set 5 m apart along the beamline. The averaged intensities and the mean energies of nuclei composing the secondary beam are listed in Table 1. The secondary beam bombarded a liquid helium

target of 100 mg/cm^2, which was contained in an aluminum cell with two windows of 6-μm Havar foil. The windows were 30 mm in diameter. The helium was condensed by a cryogenic system, and kept at approximately 4 K through the experiment. Secondary reaction products were detected using a ΔE–E telescope located at the end of the beamline, and were identified using time-of-flight (TOF), energy loss (ΔE), and energy (E) parameters. The telescope consists of nine silicon detectors of 0.5 mm thickness for ΔE, arranged in a 3 $\times$ 3 matrix, and 36 NaI(Tl) detectors [7] for E arranged in a 6 $\times$ 6 matrix. The size of each silicon detector was 50 $\times$ 50 mm^2 and each NaI(Tl) crystal had a rectangular shape of 31 $\times$ 31 $\times$ 50 mm^3. The ΔE and E detectors are arranged at 66 and 82 cm downstream from the target, respectively. The telescope was subtended at an angular range of 0–6° in the laboratory set-up. The TOF was measured between the secondary target and the NaI(Tl) scintillators. In the present experiment, the resolution for atomic and mass numbers in fluorine isotopes was 0.18 (σ) and 0.35 (σ), respectively. Scattering angles of the reaction products were measured using three parallel-plate avalanche counters (PPACs) [8]. Two PPACs were placed before the secondary target to determine the direction and the hit position on the target. The other PPAC was placed after the target to measure the direction of the reaction products. The position resolution was approximately 1 mm and the resolution of the laboratory angle was estimated to be 0.5° (σ). The effect of multiple scattering at the target was smaller than the angular resolution mentioned above. For detection of the de-excitation γ-rays from the reaction products, we used a DALI2 array of 150 NaI(Tl) detectors [9]. This surrounded the target over an angular range of 20–160° with respect to the beam axis. The typical size of the NaI(Tl) crystals was 16.0 $\times$ 8.0 $\times$ 4.0 cm^3. In the present experiment, the full-energy peak efficiency was 17.6% for 1.33-MeV γ-rays, and the energy

resolution, including insufficiency for the Doppler-shift correction, was 8.2% (σ) for 3.2-MeV γ-rays from the particle with $\beta \sim 0.27$.

Figure 1 shows γ-ray spectra obtained from the following α-induced reactions: ^{4}He(^{22}O,^{23}Fγ); ^{4}He(^{23}F,^{23}Fγ); ^{4}He(^{24}F,^{23}Fγ); and ^{4}He(^{25}Ne,^{23}Fγ). The spectra are remarkably different, indicating a strong reaction dependence of the population strengths of the excited states in ^{23}F. In these γ-ray energy spectra, we adopted a "clustering" analysis [10] to increase the full-energy peak efficiency for high-energy γ-rays. The cluster radius was chosen to be 17 cm based on a Monte-Carlo simulation, and it approximately corresponds to the distance between adjoining crystals. The full-energy peak efficiency to the 3.2-MeV γ-rays improved by approximately 50% when this analysis was adopted. The systematic error evaluated was 0.76% for γ-ray energies of the known transitions in $^{18-22}$O and $^{21-22}$F isotopes. In Fig. 1, we identified de-excitation γ-rays at 913 and 2920 keV in all the reactions, whereas observations of the other γ-rays were reaction-dependent. The peaks marked with solid circles indicate the γ-lines identified by a χ^2 test of the simulated spectra. To determine whether each γ-line originated from the γ-decay cascade in ^{23}F or not, we examined γ-ray coincidences with the γ-rays identified. As a typical example of the γ-coincidence analysis, Fig. 2 shows the γ-ray spectrum coincident with the 2920-keV γ-rays obtained from the (^{22}O,^{23}F) reactions. We identified five γ-rays at 913, 2003, 2644, 3445 and 3965 keV, identified by closed circles, which indicate the excited states at 3833, 4923, 5564, 6365 and 6905 keV in ^{23}F, respectively. A cascade of the 913- and 2920-keV γ-rays has been reported [11]. The 1245-keV γ-ray identified by an open circle, however, was found to be sequential to the 3378-keV γ-decay by analysis for coincidence γ-rays. This peak is attributed to 1245-keV photons in coincidence with the

Compton events of the 3378-keV line. The γ-coincidence analysis was also applied to all γ-rays identified in Fig. 1, and we deduced cascade γ-transitions in all the reactions.

A scheme for the levels and γ-decay proposed for the present experiment is shown in Fig. 3, together with previously reported results [11,12]. Placement of the γ-decay identified was determined based on the criterion that weaker transitions are located above stronger transitions. We observed nine new excited states, which are underlined in Fig. 3, and confirmed γ-transitions from the six excited states below the neutron separation energy at 7550 keV. To obtain the cross-sections for population of the excited states, we performed a decomposition analysis of the observed γ-ray spectra to simulated response functions of all the γ-ray sequences. The population strength of each state was evaluated as the strength parameter of a corresponding response function according to the maximum likelihood method. The systematic error of the γ-detection yield was estimated to be 9.5% from the standard source measurement. The population cross-sections deduced are shown in the bar graphs of Fig. 3 as the strength relative to the strongest population in each reaction. The largest cross-sections in the transfer, α-inelastic, one-neutron knockout and two-nucleon knockout reactions were 3.7(4) mb for the 4059-keV state, 5.5(6) mb for the 2920-keV state, 16.1(18) mb for the 2920-keV state, 1.4(3) mb for the 6629-keV state, respectively.

We specifically discuss here the proton single-particle states in the *sd* shell. Among the low-lying excited states shown in Fig. 3, the states at 2268, 3378 and 4059 keV have large cross-sections in the transfer reaction. Of the population strengths for the neutron knockout reaction, the 3378-keV state was strongly evident, but the 2268- and 4059-keV states were quite hindered. The

proton single-particle states in ^{23}F have large proton single-particle nature and little neutron-hole configuration. Therefore, the states at 2268 and 4059 keV can be strong candidates for the proton single-particle states. The ground state in ^{23}F was assigned as $5/2^+$ by Sauvan et al. [13]. We consequently assume that the $s_{1/2}$ and $d_{3/2}$ orbitals in the low-excitation-energy region contributed to the proton single-particle states in ^{23}F. It is reasonable that the 2268- and 4059-keV states correspond to the proton single-particle states in $s_{1/2}$ and $d_{3/2}$ orbitals, respectively, since the standard shell ordering in the *sd*-shell nuclei is considered to be $d_{5/2}$, $s_{1/2}$ and $d_{3/2}$.

The spin-parity assignments for these states are supported from their population strengths for the α inelastic scattering. This reaction induces core excitations and possibly populates single-particle states through non-spin-flip excitation. Thus, the proton single-particle state in the s orbital is easily excited via quadrupole excitation, but that in the d orbital has smaller population strength, since this state is considered to be mainly excited via the spin-flip process. In α inelastic scattering, the 2268-keV γ-peak was clearly identified, but the 4059-keV γ-peak was hardly observed. Therefore, the 2268- and 4059-keV states can be considered to have large proton single-particle configurations of $s_{1/2}$ and $d_{3/2}$, respectively. The two-nucleon knockout reaction was mainly used to check the consistency of the γ-decay scheme.

To confirm the s- and d-wave contributions to the 2268- and 4059-keV states, and to extract their spectroscopic factors, we compared the angular distributions of the outgoing ^{23}F particles obtained from the transfer reaction with predictions by the distorted-wave Born approximation (DWBA). Figure 4 shows the angular distributions for the 4059- and 2268-keV states, together with the predictions, assuming direct transfer of a proton into the s, d and f orbitals.

These predictions were calculated using the finite-range DWUCK5 DWBA code [14]. Optical potentials were obtained from reports by Ingemarson et al. [15,16]. The radial form factor was obtained using a wave function bound by a central potential with a spin–orbit force. The central potential was a Woods-Saxon shape, with $R = 1.25 \cdot A^{1/3}$ fm and $a = 0.65$ fm, with the well depth adjusted to give the proton binding energy. The angular distribution measured for the 4059-keV state was found to agree with the $\ell = 2$ transition. The 4059-keV state, therefore, is consistent with a proton single-particle state with $J^\pi = 3/2^+$. We deduced the spectroscopic strength $(2J_f + 1)C^2S$ of the state to be $0.95^{+0.29}_{-0.35}$, where S is a spectroscopic factor, C^2 is an isospin Clebsch-Gordan coefficient, and J_f is the total angular momentum of the investigated particle in the final channel. The error was systematically estimated from the uncertainty related to the choice of the optical potential and the experimental uncertainty in the reaction cross-sections, including the statistical error. For the 2268-keV state, the angular distribution was consistent with the prediction of $\Delta L = 0$, although we cannot completely exclude other transferred angular momenta because of statistical insufficiency. We deduced the spectroscopic strength from the angular-integrated cross-section by comparison between the measurement and the DWBA prediction. The parameters used for the DWBA calculation were the same as for the 4059-keV state. The spectroscopic strength of the 2268-keV state for $J^\pi = 1/2^+$ was deduced to be $(2J_f + 1)C^2S = 0.73^{+0.21}_{-0.33}$.

The results of the present experiment were compared with some shell model calculations for the *sd*-shell nuclei. Figure 5 shows the level schemes for ^{17}F and ^{23}F, together with predictions based on the shell model calculations for the USD [17] and SDPF-M [18,19] interactions. The experimental spectroscopic

strengths $(2J_f + 1)C^2S$ for ^{17}F were taken from Yasue et al. [20]. These shell model calculations can predict the general trend for the levels of low excitation energy. However, the proton single-particle states observed for ^{23}F are located at higher excitation energies than predicted, while other states are located at reasonable energies. In particular, according to the SDPF-M calculation, the $3/2^+_1$ state is predicted to be much lower in energy. This evidently originates from the unique modification of the monopole spin–isospin interaction in the SDPF-M interaction, which explains the appearance of the new magic number at $N = 16$ [4]. Even in the USD calculation, predictions for the excitation energy of single-particle states of $s_{1/2}$ and $d_{3/2}$ are ~500 keV lower. This result might indicate that the centroid energy gaps for $\pi d_{5/2}$–$\pi s_{1/2}$ and $\pi d_{5/2}$–$\pi d_{3/2}$ were wider than those of the predictions.

The energy gap for the $\pi d_{5/2}$–$\pi d_{3/2}$ orbitals is generated by the energy difference of their single-particle energies and effective interactions such as the monopole spin–isospin interaction. It was difficult to reproduce the observed single-particle states by tuning the strengths of the effective interactions without affecting the other low-lying excited states [19]. Therefore, we conclude that this may be attributed to an increase in the energy difference of the single-particle energies. To depict the change in single-particle energies in a simple way, we tried to calculate the energies of the excited states in ^{23}F using the shell model code OXBASH [21] based on the USD interaction and tuning the single-particle energies of the $d_{5/2}$ and $d_{3/2}$ orbitals. When the single-particle energy of $\pi d_{5/2}$ was reduced by 0.48 MeV and that of $\pi d_{3/2}$ was increased by 0.72 MeV, the excitation energies of the proton single-particle states $1/2^+_1$ and $3/2^+_1$ were 2111 and 4116 keV, respectively, although the other excited states did not change much. The spin–orbit interaction is a nuclear surface effect,

and is given by a derivative of the nuclear central potential [22]. Thus, the spin–orbit splitting is naively considered to be determined by the depth of the potential, and to be sensitive to the binding energy of the valence proton. In the present case, the valence proton in ^{23}F is much more deeply bound ($\sim$13.0 MeV) than in ^{17}F ($\sim$0.6 MeV). Therefore, this difference in binding energy may cause the spin–orbit splitting of single-particle energies in ^{23}F to be greater than in ^{17}F.

The authors thank the RIKEN Ring Cyclotron staff for cooperation during the experiment. They wish to acknowledge helpful discussions with T. Otsuka and Y. Utsuno. One of the authors (S.M.) is grateful for financial assistance from the Special Postdoctoral Researcher Program of RIKEN. The present work was partially supported by a Grant-In-Aid for Scientific Research from the Japan Ministry of Education, Culture, Sports, Science and Technology under program number (A) 15204018.

References

[1] A. Ozawa et al., Phys. Rev. Lett. 84 (2000) 5493.

[2] H. Sakurai et al., Phys. Lett. 448B (1999) 180.

[3] E.K. Warburton et al., Phys. Rev. C 41 (1990) 1147.

[4] T. Otsuka et al., Phys. Rev. Lett. 87 (2001) 082502.

[5] H. Ryuto et al., Nucl. Instrum. Methods A, in print.

[6] T. Kubo et al., Nucl. Instrum. Methods B 70 (1992) 322.

[7] M. Tamaki et al., CNS-REP-59 (2003) 76.

[8] S. Kumagai et al., Nucl. Instrum. Methods A 470 (2001) 562.

[9] S. Takeuchi et al., RIKEN Accel. Prog. Rep. 36 (2003) 148.

[10] K. Yamada et al., Phys. Lett. 579B (2004) 265.

[11] M. Belleguic et al., Nucl. Phys. A682 (2001) 136c.

[12] N.A. Orr et al., Nucl Phys. A491 (1989) 457.

[13] E. Sauvan et al., Phys. Lett. 491B (2000) 1.

[14] P.D. Kunz computer code DWUCK5, *unpublished.*

[15] A. Ingemarson et al., Nucl. Phys. A676 (2000) 3.

[16] A. Ingemarson et al., Nucl. Phys. A696 (2001) 3.

[17] B.H. Wildenthal Prog. Part. Nucl. Phys. 11 (1984) 5.

[18] Y. Utsuno et al., Phys. Rev. C 64 (1999) 011301.

[19] T. Otsuka Y. Utsuno, *private communication.*

[20] M. Yasue et al., Phys. Rev. C 46 (1992) 1242.

[21] B.A. Brown et al., OXBASH, Michigan State University Cyclotron Laboratory, Report No. 524, 1986.

[22] A. Bohr, B.R. Mottelson, in: Nuclear Structure, Vol. I, W.A. Benjamin, 1975.

Table 1

Composition of the secondary beam.

Nuclide	^{22}O	^{23}F	^{24}F	^{25}Ne
Energy (AMeV)	35.0	41.5	36.0	42.7
Intensity (particles/s)	2.0×10^3	5.5×10^2	4.7×10^2	1.2×10^3
Flux (%)	40	11	10	23

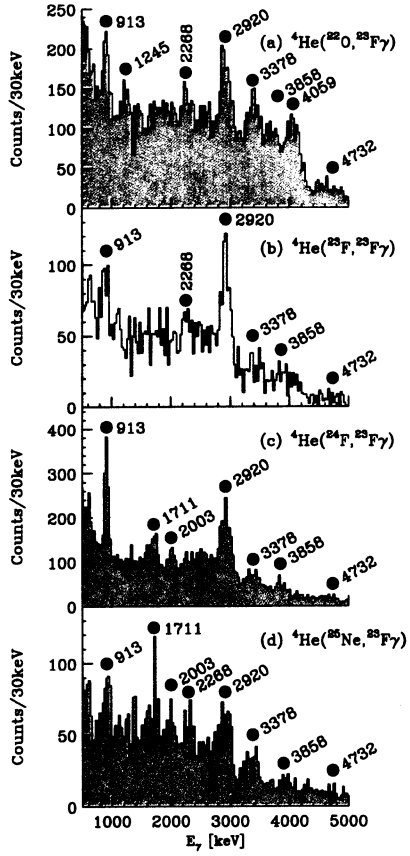

Fig. 1. Doppler-corrected γ-ray spectra for four different reactions: (a) proton transfer reaction ^{4}He(^{22}O,^{23}Fγ); (b) inelastic scattering ^{4}He(^{23}F,^{23}Fγ); (c) neutron-knockout reaction ^{4}He(^{24}F,^{23}Fγ); and (d) two-nucleon knockout reaction ^{4}He(^{25}Ne,^{23}Fγ).

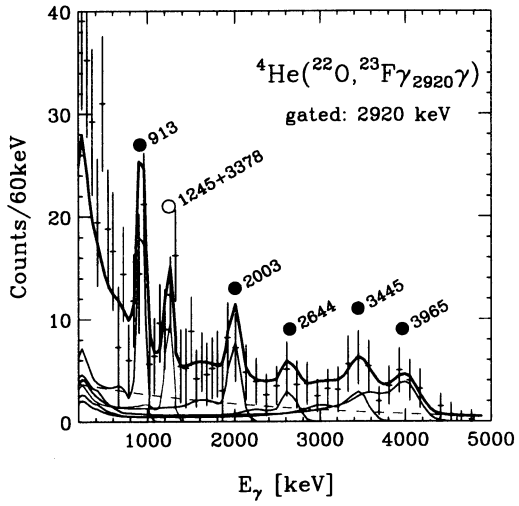

Fig. 2. γ-Ray spectrum for the transfer reaction ^{4}He(^{22}O,^{23}F) in coincidence with the 2920-keV γ-ray. The thin solid curves show response functions of the γ-ray detector array for each of the γ-lines, which were calculated by Monte-Carlo simulation, and the dashed curve shows the exponential background. The thick solid curve shows the summation of these thin solid and dashed curves. The closed circles indicate γ-lines coincident with the 2920-keV γ-ray, and the open circle indicates the γ-line corresponding to the sequential γ-decay of the 3378- and 1245-keV lines. See text for details.

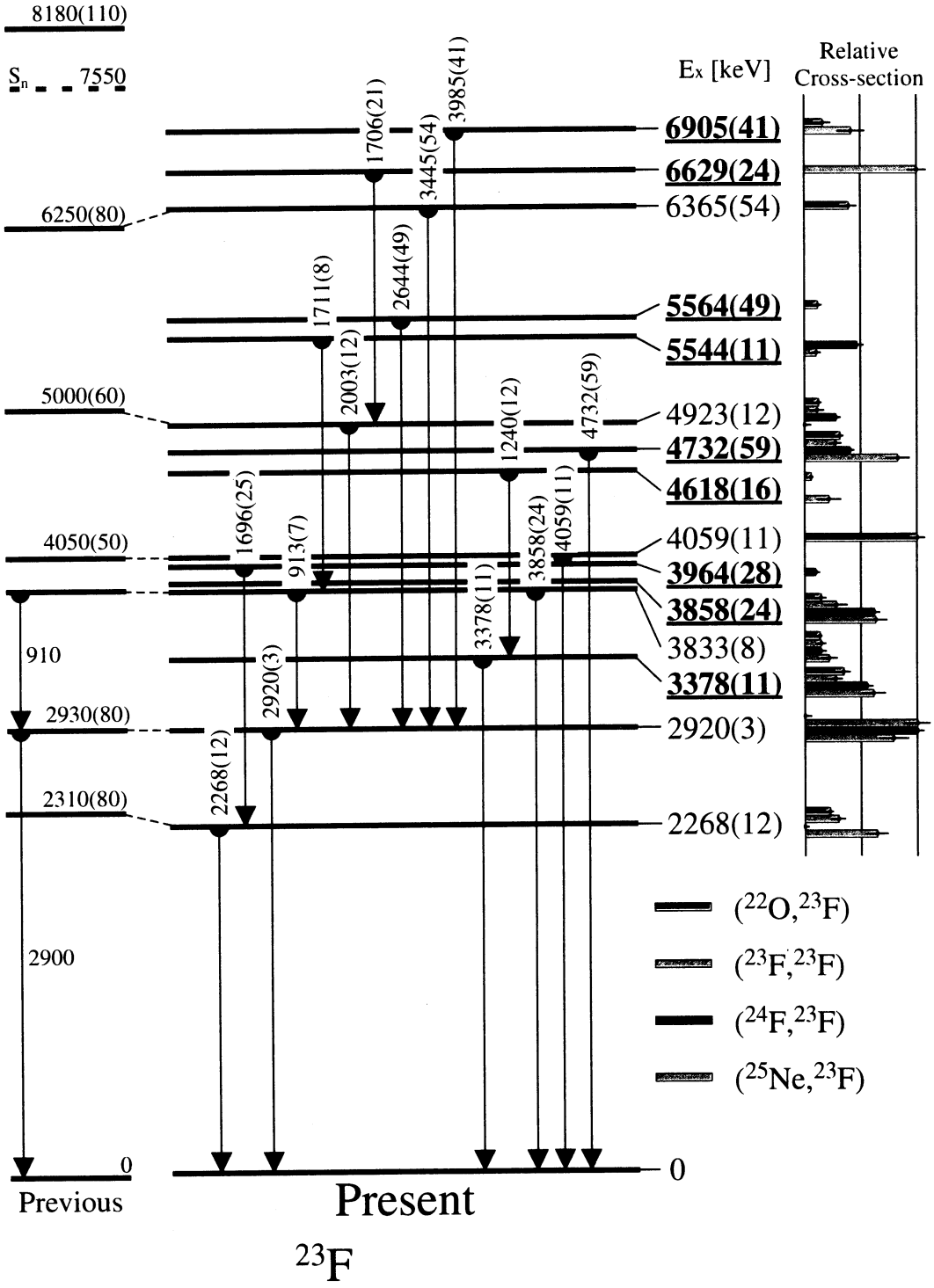

Fig. 3. Proposed scheme for the levels and γ-decay in ^{23}F, together with previous results. Underlined energy levels indicate excited levels newly observed in the present experiment. The bars to the right of the excitation energies show the relative cross-sections for these states. The errors shown with γ-ray energies, excitation energies and relative cross-sections are statistical errors obtained by fitting of the γ-ray spectra with the simulated response functions of DALI2.

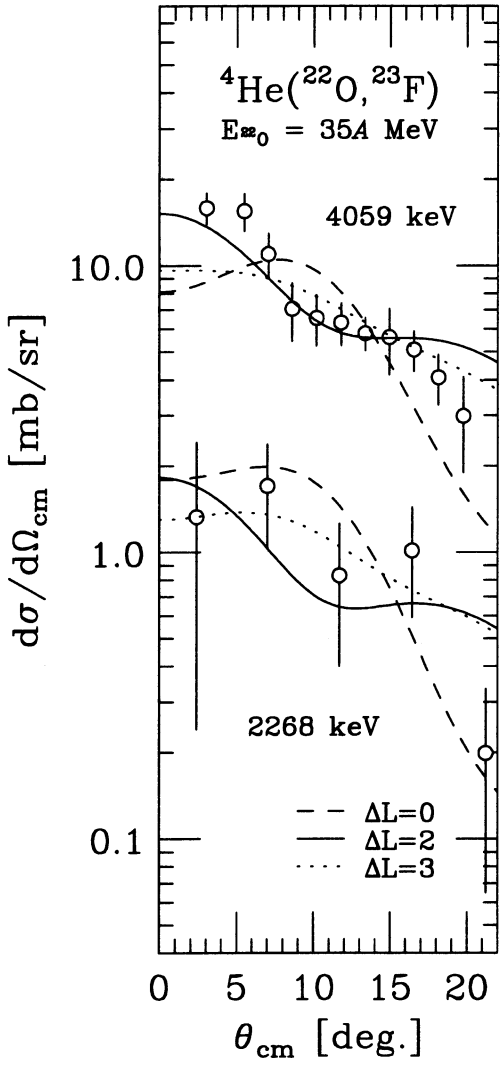

Fig. 4. Angular distributions for the 2268- and 4059-keV states from the proton transfer reaction, together with DWBA predictions. The angular distributions for the 4059- and 2268-keV states are shown in the upper and lower plots of the figure, respectively. The dashed, solid and dotted lines indicate the DWBA predictions for transferred angular momenta of ΔL = 0, 2 and 3, respectively. The DWBA lines were obtained using the optical potential parameters reported by Ingemarson et al. [15,16], taking into account the angular resolution of the detectors.

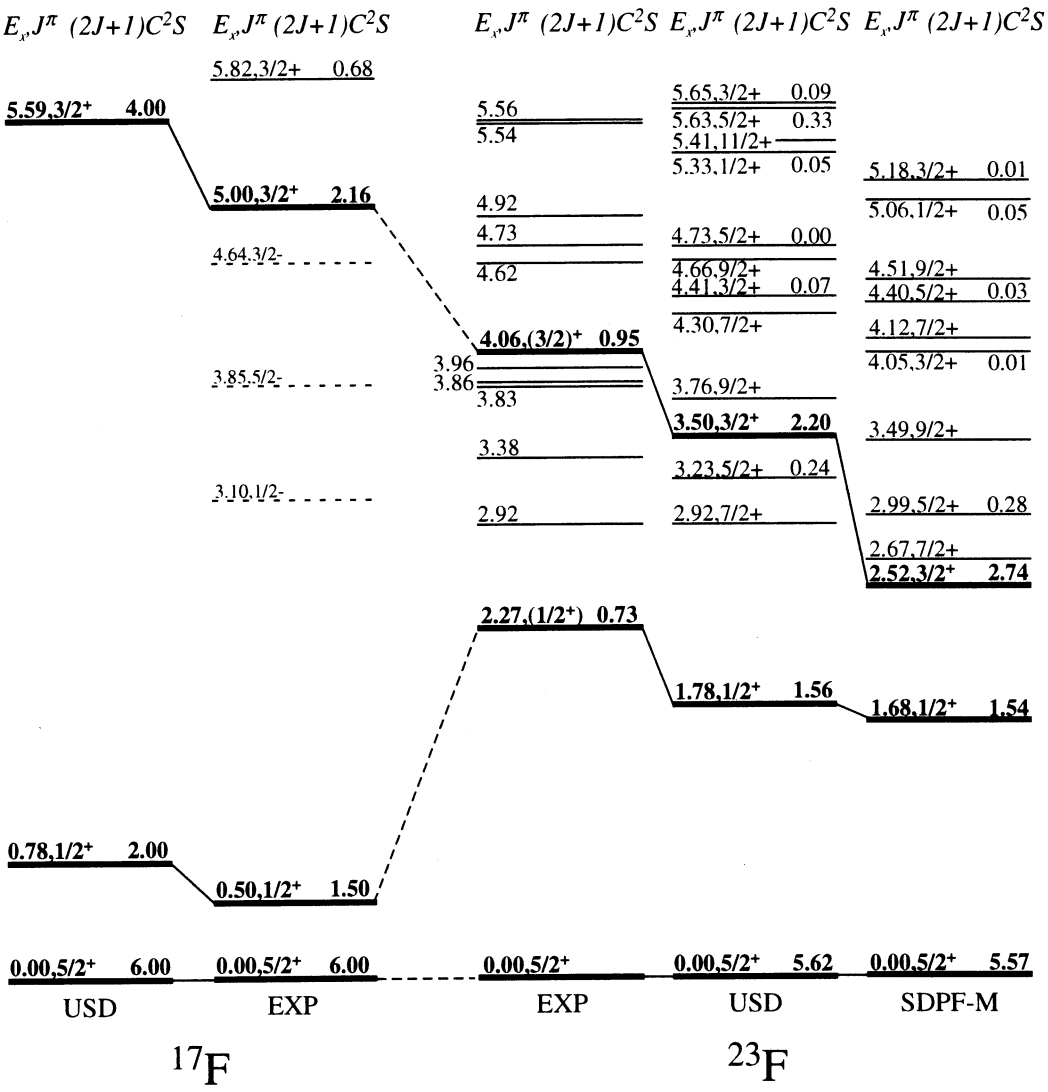

Fig. 5. Level schemes for ^{17}F and ^{23}F, together with the shell model calculations using USD [17] and SDPF-M [18,19] interactions. The experimental spectroscopic strengths for ^{17}F reported by Yasue et al. [20] were used as references.